Non-Proprietary Version

Materials Reliability Program Generic Evaluation of Examination Coverage Requirements for Reactor Pressure Vessel Head Penetration Nozzles, Revision 1 (MRP-95R1NP)

1011225

Topical Report, September 2004

NON-PROPRIETARY INFORMATION

NOTICE: This report contains the non-proprietary information that is included in the proprietary version of this report. The proprietary version of this report contains proprietary information that is the intellectual property of MRP utility members and EPRI. Accordingly, the proprietary versions are only available under license from EPRI and may not be reproduced or disclosed, wholly or in part, by any Licensee to any other person or organization.

EPRI Project Manager
C. King

EPRI • 3412 Hillview Avenue, Palo Alto, California 94304 • PO Box 10412, Palo Alto, California 94303 • USA
800.313.3774 • 650.855.2121 • askepri@epri.com • www.epri.com

DISCLAIMER OF WARRANTIES AND LIMITATION OF LIABILITIES

THIS DOCUMENT WAS PREPARED BY THE ORGANIZATION(S) NAMED BELOW AS AN ACCOUNT OF WORK SPONSORED OR COSPONSORED BY THE ELECTRIC POWER RESEARCH INSTITUTE, INC. (EPRI). NEITHER EPRI, ANY MEMBER OF EPRI, ANY COSPONSOR, THE ORGANIZATION(S) BELOW, NOR ANY PERSON ACTING ON BEHALF OF ANY OF THEM:

(A) MAKES ANY WARRANTY OR REPRESENTATION WHATSOEVER, EXPRESS OR IMPLIED, (I) WITH RESPECT TO THE USE OF ANY INFORMATION, APPARATUS, METHOD, PROCESS, OR SIMILAR ITEM DISCLOSED IN THIS DOCUMENT, INCLUDING MERCHANTABILITY AND FITNESS FOR A PARTICULAR PURPOSE, OR (II) THAT SUCH USE DOES NOT INFRINGE ON OR INTERFERE WITH PRIVATELY OWNED RIGHTS, INCLUDING ANY PARTY'S INTELLECTUAL PROPERTY, OR (III) THAT THIS DOCUMENT IS SUITABLE TO ANY PARTICULAR USER'S CIRCUMSTANCE; OR

(B) ASSUMES RESPONSIBILITY FOR ANY DAMAGES OR OTHER LIABILITY WHATSOEVER (INCLUDING ANY CONSEQUENTIAL DAMAGES, EVEN IF EPRI OR ANY EPRI REPRESENTATIVE HAS BEEN ADVISED OF THE POSSIBILITY OF SUCH DAMAGES) RESULTING FROM YOUR SELECTION OR USE OF THIS DOCUMENT OR ANY INFORMATION, APPARATUS, METHOD, PROCESS, OR SIMILAR ITEM DISCLOSED IN THIS DOCUMENT.

ORGANIZATION(S) THAT PREPARED THIS DOCUMENT

Structural Integrity Associates

ORDERING INFORMATION

Requests for copies of this report should be directed to EPRI Orders and Conferences, 1355 Willow Way, Suite 278, Concord, CA 94520, (800) 313-3774, press 2 or internally x5379, (925) 609-9169, (925) 609-1310 (fax).

Electric Power Research Institute and EPRI are registered service marks of the Electric Power Research Institute, Inc. EPRI. ELECTRIFY THE WORLD is a service mark of the Electric Power Research Institute, Inc.

Copyright © 2004 Electric Power Research Institute, Inc. All rights reserved.

CITATIONS

This report was prepared by

Structural Integrity Associates
6595 S. Dayton St. (Suite 3000)
Greenwood Village, CO 80111

Principal Investigator
P. Riccardella

This report describes research sponsored by EPRI.

The report is a corporate document that should be cited in the literature in the following manner:

Materials Reliability Program: Generic Evaluation of Examination Coverage Requirements for Reactor Pressure Vessel Head Penetration Nozzles, Revision 1 (MRP-95R1NP), EPRI, Palo Alto, CA: 2004. 1011225.

PRODUCT DESCRIPTION

U.S. NRC Revised Order EA-03-009 issued on February 20, 2004 requires specific examinations of the reactor pressure vessel (RPV) top head and vessel head penetration nozzles of all pressurized water (PWR) plants. The MRP has developed an alternative head inspection plan based on a comprehensive RPV top head safety assessment. This report contains a generic technical justification of the inspection zone contained in the MRP inspection plan.

Results & Findings

The results of this evaluation support an inspection zone corresponding to a right circular cylinder extending from 1 inch above the highest point of the root of the J-groove weld to 1 inch below the lowest point of the toe of the weld for large angle CRDM and CEDM nozzles (>30°). For smaller angle nozzles (≤30°) and ICI nozzles, the cylinder extends from 1.5 inches above the highest point of the root of the J-groove weld to 1.5 inches below the lowest point of the toe of the weld.

The report establishes a reasonable target stress value (20 ksi tension), below which the probability of PWSCC is extremely remote, and demonstrates that, in all but a few isolated cases, the inspection zone, as defined above, envelopes all locations with stresses above this stress level. In no case does the examination zone exclude locations with stresses higher than 20.3 ksi. The report also includes PWSCC growth calculations of postulated flaws that could be overlooked due to unexamined regions, to demonstrate that such flaws, either above or below the weld, would not grow to unacceptable sizes in the time period until the next inspection required by the MRP inspection plan. Finally, review of prior plant inspection data from a large cross-section of U.S. PWRs revealed that, of 237 flaw indications reported in these inspections, all flaws would have been detected had the inspections been limited to just the above examination zone.

Challenges & Objectives

This study's objective was to determine a practical examination zone that provides an acceptable level of quality and safety for all U.S. PWR RPV upper vessel head penetration nozzles.

Applications, Values & Use

The evaluation considers stresses in a group of characteristic plants that reasonably bound the fleet of U.S. PWRs from the standpoint of important factors that contribute to nozzle residual and operating stresses.

EPRI Perspective

This project has determined a practical examination zone for PWR RPV upper vessel head penetration nozzles that provides an acceptable level of quality and safety. A review of prior plant inspection data revealed that all flaws detected to date in top head nozzle exams in U.S. PWRs would have been detected had the inspections been limited to just the proposed examination zones.

Approach

The project team developed plots of stress versus distance above and below the J-groove weld for several nozzles in four plants that reasonably bound the U.S. PWR fleet in terms of parameters that are expected to affect top head nozzle residual and operating stresses. The team then defined inspection zones, beyond which stresses decay significantly to levels at which PWSCC is considered highly unlikely. Then, assuming (non-mechanistically) that cracks form in the uninspected regions up to and impinging on the proposed inspection zones, the team performed fracture mechanics calculations to demonstrate that such cracks would not propagate to an unacceptable size in the time period until the next required inspections. These calculations were completed for plants of various RPV head designs and operating temperatures. Finally, nondestructive examination (NDE) data are reviewed and presented to demonstrate that in no case in which top head nozzle cracking has been detected would inspections of the proposed examination zones have missed such cracking.

Keywords

Primary water stress corrosion cracking
PWSCC
Alloy 600
Alloy 82/182
CRDM Nozzle
CEDM Nozzle
RPV Head penetration
J-groove weld

CONTENTS

1 **INTRODUCTION** **1-1**

2 **STRESS EVALUATION** **2-1**

2.1 Stress Limit for Examination Zone Definition 2-1

2.2 Characteristic Plants for Evaluation 2-1

2.3 Stress Plots and Determination of Limit Stress Distances 2-2

3 **EXAMINATION ZONES** **3-1**

4 **FRACTURE MECHANICS ANALYSES** **4-1**

4.1 Growth of Axial Cracks Below the Weld 4-1

4.2 Growth of Circumferential Cracks Above the Weld 4-5

5 **COMPARISON TO PAST INSPECTION RESULTS** **5-1**

6 **CONCLUSIONS** **6-1**

7 **REFERENCES** **7-1**

A **APPENDIX A** **A-1**

LIST OF FIGURES

Figure 2-1 Typical pattern of RPV Top Head Nozzle Stresses Above and Below the J-Groove Weld (Steepest Angle Nozzle in a B&W-type Plant) 2-3
Figure 2-2 Comparison of Key Weld Geometry Variables Influencing Nozzle Residual Stresses – Plants Evaluated in this Study are Labeled 2-4
Figure 3-1 Illustration of RPV Top Head Nozzle Inspection Zone 3-4
Figure 4-1 Illustration of Assumed Axial Flaw and Permissible Crack Growth Below the Weld Inspection Zone 4-9
Figure 4-2 Illustration of Assumed Circumferential Flaws Above the Weld Inspection Zone 4-10
Figure 4-3 Envelope Stresses Compared to Stresses at Edge of Inspection Zone 4-11
Figure 5-1 Flaw Area Outside of Weld 5-2

Figure A-1 Plant A (B&W) 38º Nozzle downhill Hoop Stress A-2
Figure A-2 Plant A (B&W) 38º Nozzle downhill Axial Stress A-2
Figure A-3 Plant A (B&W) 38º Nozzle sidehill Hoop Stress A-3
Figure A-4 Plant A (B&W) 38º Nozzle sidehill Axial Stress A-3
Figure A-5 Plant A (B&W) 38º Nozzle uphill Hoop Stress A-4
Figure A-6 Plant A (B&W) 38º Nozzle uphill Axial Stress A-4
Figure A-7 Plant A (B&W) 26º Nozzle downhill Hoop Stress A-5
Figure A-8 Plant A (B&W) 26º Nozzle downhill Axial Stress A-5
Figure A-9 Plant A (B&W) 26º Nozzle sidehill Hoop Stress A-6
Figure A-10 Plant A (B&W) 26º Nozzle sidehill Axial Stress A-6
Figure A-11 Plant A (B&W) 26º Nozzle uphill Hoop Stress A-7
Figure A-12 Plant A (B&W) 26º Nozzle uphill Axial Stress A-7
Figure A-13 Plant A (B&W) 18º Nozzle downhill Hoop Stress A-8
Figure A-14 Plant A (B&W) 18º Nozzle downhill Axial Stress A-8
Figure A-15 Plant A (B&W) 18º Nozzle sidehill Hoop Stress A-9
Figure A-16 Plant A (B&W) 18º Nozzle sidehill Axial Stress A-9
Figure A-17 Plant A (B&W) 18º Nozzle uphill Hoop Stress A-10
Figure A-18 Plant A (B&W) 18º Nozzle uphill Axial Stress A-10
Figure A-19 Plant A (B&W) 0º Nozzle downhill Hoop Stress A-11
Figure A-20 Plant A (B&W) 0º Nozzle downhill Axial Stress A-11
Figure A-21 Plant A (B&W) 0º Nozzle sidehill Hoop Stress A-12

Figure A-22 Plant A (B&W) 0º Nozzle sidehill Axial Stress A-12
Figure A-23 Plant A (B&W) 0º Nozzle uphill Hoop Stress A-13
Figure A-24 Plant A (B&W) 0º Nozzle uphill Axial Stress A-13
Figure A-25 Plant B (Westinghouse 2-loop) 43º Nozzle downhill Hoop Stress A-14
Figure A-26 Plant B (Westinghouse 2-loop) 43º Nozzle downhill Axial Stress A-14
Figure A-27 Plant B (Westinghouse 2-loop) 43º Nozzle sidehill Hoop Stress A-15
Figure A-28 Plant B (Westinghouse 2-loop) 43º Nozzle sidehill Axial Stress A-15
Figure A-29 Plant B (Westinghouse 2-loop) 43º Nozzle uphill Hoop Stress A-16
Figure A-30 Plant B (Westinghouse 2-loop) 43º Nozzle uphill Axial Stress A-16
Figure A-31 Plant B (Westinghouse 2-loop) 30º Nozzle downhill Hoop Stress A-17
Figure A-32 Plant B (Westinghouse 2-loop) 30º Nozzle downhill Axial Stress A-17
Figure A-33 Plant B (Westinghouse 2-loop) 30º Nozzle sidehill Hoop Stress A-18
Figure A-34 Plant B (Westinghouse 2-loop) 30º Nozzle sidehill Axial Stress A-18
Figure A-35 Plant B (Westinghouse 2-loop) 30º Nozzle uphill Hoop Stress A-19
Figure A-36 Plant B (Westinghouse 2-loop) 30º Nozzle uphill Axial Stress A-19
Figure A-37 Plant B (Westinghouse 2-loop) 13º Nozzle downhill Hoop Stress A-20
Figure A-38 Plant B (Westinghouse 2-loop) 13º Nozzle downhill Axial Stress A-20
Figure A-39 Plant B (Westinghouse 2-loop) 13º Nozzle sidehill Hoop Stress A-21
Figure A-40 Plant B (Westinghouse 2-loop) 13º Nozzle sidehill Axial Stress A-21
Figure A-41 Plant B (Westinghouse 2-loop) 13º Nozzle uphill Hoop Stress A-22
Figure A-42 Plant B (Westinghouse 2-loop) 13º Nozzle uphill Axial Stress A-22
Figure A-43 Plant B (Westinghouse 2-loop) 0º Nozzle downhill Hoop Stress A-23
Figure A-44 Plant B (Westinghouse 2-loop) 0º Nozzle downhill Axial Stress A-23
Figure A-45 Plant B (Westinghouse 2-loop) 0º Nozzle sidehill Hoop Stress A-24
Figure A-46 Plant B (Westinghouse 2-loop) 0º Nozzle sidehill Axial Stress A-24
Figure A-47 Plant B (Westinghouse 2-loop) 0º Nozzle uphill Hoop Stress A-25
Figure A-48 Plant B (Westinghouse 2-loop) 0º Nozzle uphill Axial Stress A-25
Figure A-49 Plant C (Westinghouse 4-loop) 48º Nozzle downhill Hoop Stress A-26
Figure A-50 Plant C (Westinghouse 4-loop) 48º Nozzle downhill Axial Stress A-26
Figure A-51 Plant C (Westinghouse 4-loop) 48º Nozzle sidehill Hoop Stress A-27
Figure A-52 Plant C (Westinghouse 4-loop) 48º Nozzle sidehill Axial Stress A-27
Figure A-53 Plant C (Westinghouse 4-loop) 48º Nozzle uphill Hoop Stress A-28
Figure A-54 Plant C (Westinghouse 4-loop) 48º Nozzle uphill Axial Stress A-28
Figure A-55 Plant D (CE) 49º Nozzle downhill Hoop Stress A-29
Figure A-56 Plant D (CE) 49º Nozzle downhill Axial Stress A-29
Figure A-57 Plant D (CE) 49º Nozzle sidehill Hoop Stress A-30
Figure A-58 Plant D (CE) 49º Nozzle sidehill Axial Stress A-30
Figure A-59 Plant D (CE) 49º Nozzle uphill Hoop Stress A-31
Figure A-60 Plant D (CE) 49º Nozzle uphill Axial Stress A-31

Figure A-61 Plant D (CE) 8º Nozzle downhill Hoop Stress A-32
Figure A-62 Plant D (CE) 8º Nozzle downhill Axial Stress A-32
Figure A-63 Plant D (CE) 8º Nozzle sidehill Hoop Stress A-33
Figure A-64 Plant D (CE) 8º Nozzle sidehill Axial Stress A-33
Figure A-65 Plant D (CE) 8º Nozzle uphill Hoop Stress A-34
Figure A-66 Plant D (CE) 8º Nozzle uphill Axial Stress A-34
Figure A-67 Plant D (CE) ICI Nozzle downhill Hoop Stress A-35
Figure A-68 Plant D (CE) ICI Nozzle downhill Axial Stress A-35
Figure A-69 Plant D (CE) ICI Nozzle sidehill Hoop Stress A-36
Figure A-70 Plant D (CE) ICI Nozzle sidehill Axial Stress A-36
Figure A-71 Plant D (CE) ICI Nozzle uphill Hoop Stress A-37
Figure A-72 Plant D (CE) ICI Nozzle uphill Axial Stress A-37

LIST OF TABLES

Table 3-1 Evaluation of Stresses at Top Edge of Above-Weld Inspection Zone in Characteristic Plants 3-2

Table 3-2 Evaluation of Stresses at Bottom Edge of Below-Weld Inspection Zone in Characteristic Plants 3-3

Table 4-1 Starting Flaw Lengths for Crack Growth Analysis of Postulated Axial Cracks below J-Groove Welds 4-2

Table 4-2 Crack Growth Times for Postulated Axial Cracks at Edge of Below Weld Inspection Zone to Reach Weld (Minimum Time is Greater than Fifteen EFPYs) 4-4

Table 4-3 Stress Intensity Factor for Above-Weld Circumferential Flaws for Plant A (B&W Type Plant - 38° Nozzle - Envelop Stress Distributions) 4-6

Table 4-4 Stress Intensity Factor for Above-Weld Circumferential Flaws for Plant B (W 2-Loop Plant - 43.5º Nozzle - Envelop Stress Distributions) 4-6

Table 4-5 Stress Intensity Factor for Above-Weld Circumferential Flaws for Plant C (W 4-Loop Plant – 48.8º Nozzle - Envelop Stress Distributions) 4-7

Table 4-6 Stress Intensity Factor for Above-Weld Circumferential Flaws for Plant D (CE Plant – 49.7º Nozzle - Envelop Stress Distributions) 4-7

Table 4-7 Growth Time from 30° to 300° Circumferential Cracks in Limiting Nozzles in Four Characteristic Plants (Assumed top head temperature = 600°F) 4-8

1
INTRODUCTION

U.S. NRC Revised Order EA-03-009 issued on February 20, 2004 [1] requires specific examinations of the reactor pressure vessel (RPV) top head and vessel head penetration nozzles of all pressurized water (PWR) plants. In accordance with the order, inspections are required to be performed at various intervals, depending on the susceptibility ranking of the individual plants. The scope of the required inspections consists of:

(a) Bare metal visual (BMV) examination of 100% of the RPV head surface (including 360° around each RPV head penetration nozzle), with an allowance for heads with some portions of the surface obscured by support structures to only inspect 95%, subject to certain provisions, AND

(b) Either:

(i) Ultrasonic testing of each RPV head penetration nozzle (i.e. nozzle base material) from two (2) inches above the highest point of the root of the J-groove weld (on a horizontal plane perpendicular to the nozzle axis) to two (2) inches below the lowest point at the toe of the J-groove weld on a horizontal plane perpendicular to the nozzle axis (or the bottom of the nozzle if less than 2 inches). The inspection zone below the J-groove weld can be reduced to one (1) inch below the lowest point at the toe of the J-groove weld (on a horizontal plane perpendicular to the nozzle axis) plus all portions of the nozzle surfaces below the J-groove weld that have an operating stress of 20 ksi tension or greater. In addition, an assessment shall be made to determine if leakage has occurred into the annulus between the RPV head penetration nozzle and the RPV head low alloy steel., OR

(ii) Eddy current testing or dye penetrant testing of the entire wetted surface of each J-groove weld and the same zones of the RPV head penetration nozzle base material as described in (i) above..

The MRP has developed an alternative head inspection plan [2] based on a comprehensive RPV top head safety assessment [3] that considers all possible sources and consequences of RPV top head nozzle degradation. The safety assessment has been submitted to the NRC for approval, and the alternative head inspection plan and its technical basis are under consideration by the ASME Section XI Code committee on nuclear inservice inspection for revision to the ASME Section XI requirements for head inspections.

The recommended inspection zone for top head penetrations in the MRP alternative inspection plan [2] is different than the inspection zone requirements in the NRC order summarized above. This report contains a generic technical justification for the revised inspection zone requirements contained in the MRP inspection plan. It addresses extent of examination both above the top and below the bottom of the J-groove weld. The evaluation includes stress analysis, fracture mechanics analysis and a review of prior inspection data to demonstrate that the probability of PWSCC initiating in regions not included in the inspection zone is extremely remote, and that even if such cracking were to initiate, it would not propagate to a size that would lead to leakage or nozzle failure in the time period until the next inspections required by the plan.

Stresses are summarized from prior analyses of a group of characteristic plants that are shown to bound the fleet of U.S. PWRs from the standpoint of the important factors that contribute to nozzle residual and operating stresses. Plots of stress versus distance above and below the J-groove weld are then developed for several nozzles (of various incidence angle with the heads) in these plants. Inspection zones are then defined, beyond which the stresses decay significantly, to levels at which primary water stress corrosion cracking (PWSCC) is considered highly unlikely (i.e. ≤ 20 ksi tension stress). Then, assuming (non-mechanistically) that cracks form in the uninspected regions up to and impinging upon the proposed inspection zones, fracture mechanics calculations are performed to demonstrate that such cracks would not propagate to an unacceptable size in the characteristic plant nozzles. Finally, NDE data are reviewed and presented to demonstrate the effectiveness of the proposed examination zone with respect to prior inspection results for U.S. PWR top head nozzles.

2
STRESS EVALUATION

2.1 Stress Limit for Examination Zone Definition

PWSCC in RPV head nozzles occurs due to a combination of susceptible materials, environment and high stress levels. In the vicinity of the J-groove welds, where the cracking has been observed, high stresses generally exist due to welding residual stresses, plus a small contribution from operating thermal and pressure stresses. Typical plots of operating plus residual stresses for a top head penetration nozzle are illustrated in Figure 2-1. This figure presents hoop stresses on the nozzle inside and outside surfaces, as a function of axial distance from the bottom of the nozzle (located at 64.5 inches on the horizontal axis). The upper chart (a) is for the uphill side of the nozzle, while the lower plot (b) is for the downhill side. Weld locations are identified by rectangular boxes on these charts. It is seen from this figure that the stresses peak at values on the order of 80 ksi directly under the welds, but that they attenuate rapidly with distance either above or below the weld.

In order to determine a practical examination zone that will ensure an acceptable level of quality and safety, it is desirable to define a stress limit below which there is a very low probability of initiating PWSCC cracks. There is fairly universal agreement that high stresses, on the order of the material yield strength, are necessary to initiate PWSCC. Reference [4] states "there is no known case of stress corrosion cracking of Alloy-600 below the yield stress." Typical yield strengths for wrought Alloy-600 head penetration nozzles are in the range of 37 ksi to 65 ksi. (The ASME Code minimum yield strength is 35 ksi for SB-166 material, and 30 ksi for SB-167 hot worked tube material.) Weld metal yield strengths are generally higher. For purposes of this evaluation, a target stress level of 20 ksi tension has been selected as a safe value, below which PWSCC initiation is very unlikely.

2.2 Characteristic Plants for Evaluation

A group of characteristic plants have been selected for evaluation that bound the U.S. PWR fleet in terms of parameters that affect top head nozzle residual and operating stresses. The specific plant types selected are:

- Plant A – A typical B&W type plant with nozzle angles ranging from 0° to 38°, and reported nozzle yield strengths ranging from 36.8 to 50 ksi. [5]
- Plant B – A Westinghouse 2-loop plant with nozzle angles ranging from 0° to 43.5°, and reported nozzle yield strength of 58 ksi. [6]

- Plant C – A Westinghouse 4-loop plant with nozzle angles ranging from 0° to 48.8°, and reported nozzle yield strength of 63 ksi. [8]
- Plant D – A large CE type plant with CEDM nozzle angles ranging from 0° to 49.7°, and reported nozzle yield strengths ranging from 52.5 to 59 ksi. This plant also contained ICI nozzles with a 55.3° nozzle angle and a yield strength of 39.5 ksi.[8]

In addition to nozzle angle and yield strength, an important factor influencing residual stress is the weld geometry. Figure 2-2 summarizes a wide range of PWR top head nozzle geometries which have been previously analyzed, encompassing 51 of the 69 U.S. PWRs. Plotted on the horizontal axis of this chart is the average J-groove weld cross-sectional area for each of the plants, distinguished by ranges of nozzle angle. Plotted on the vertical axis is the ratio of uphill to downhill weld cross-sectional area for the same nozzles. In general, the larger the weld size, the higher the residual stress one would expect. The ratio of uphill to downhill weld areas is also expected to effect the distribution of stress around the nozzle, and the stress attenuation with distance from the weld. Data points representing the nozzles analyzed in the four characteristic plant types listed above are shown in red and labeled in this chart. It is seen from Figure 2-2 that the four plants selected bound the complete range of plants analyzed in terms of largest weld size and the ratio of uphill to downhill weld sizes. Plant B represents the largest average weld size in the group, and also has relatively high yield strength. Plants A and C have about average weld sizes but span the range of uphill to downhill weld size ratios, from the highest (uphill weld area almost twice that of the downhill weld) to the lowest (downhill weld area more than twice that of the uphill weld). Plant D is somewhat central to the group, both in terms of average weld size and ratio. This group of plants also spans a wide range of nozzle yield strengths, from 36.8 ksi to 63 ksi. In addition to the highest angle nozzles for each plant, the evaluation also addresses selected intermediate and low angle welds from several of the plant types, as well as ICI nozzles in the CE type plant, to cover the full range of possible nozzles.

The conclusion of this study is that the characteristic plants selected for evaluation bound the fleet of U.S. plants in terms of weld geometries and yield strengths and therefore residual stresses, and that the resulting examination zone definition based on these stresses is applicable to all U.S. PWRs.

2.3 Stress Plots and Determination of Limit Stress Distances

Stress plots similar to Figure 2-1 have been obtained from prior calculations [5 – 8] for the maximum angle nozzle in each of the four characteristic plants, as well as for several intermediate angle nozzles from the same plants. The complete series of plots, including hoop and axial stresses for uphill, sidehill, and downhill locations in each nozzle are compiled in Appendix A. These plots were used to determine the distances above and below the weld at which the stress decays to below the 20 ksi tension limit. The results are summarized and used as the basis for defining an examination zone in Section 3 below.

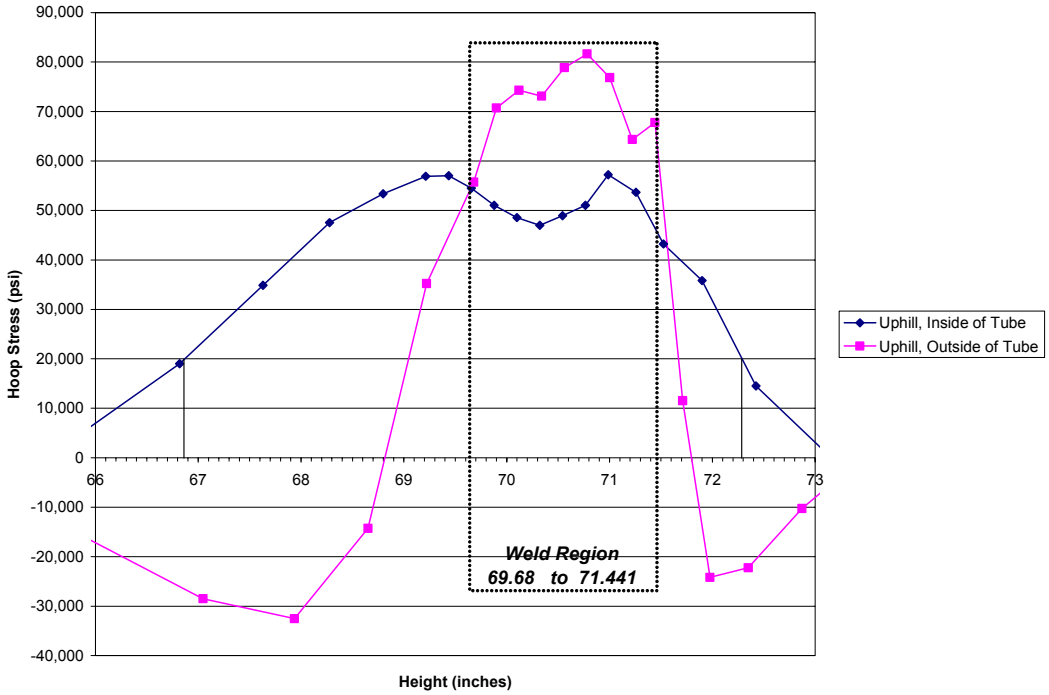

(a) Uphill Side of Nozzle

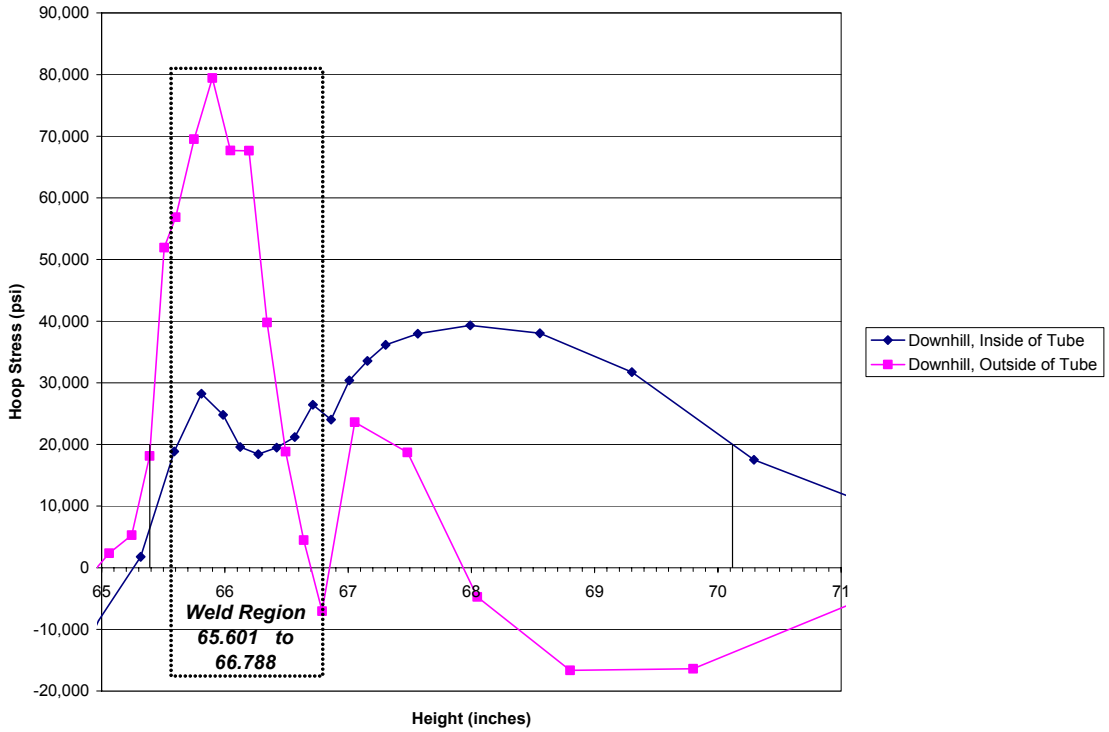

(b) Downhill side of Nozzle

Figure 2-1
Typical pattern of RPV Top Head Nozzle Stresses Above and Below the J-Groove Weld (Steepest Angle Nozzle in a B&W-type Plant)

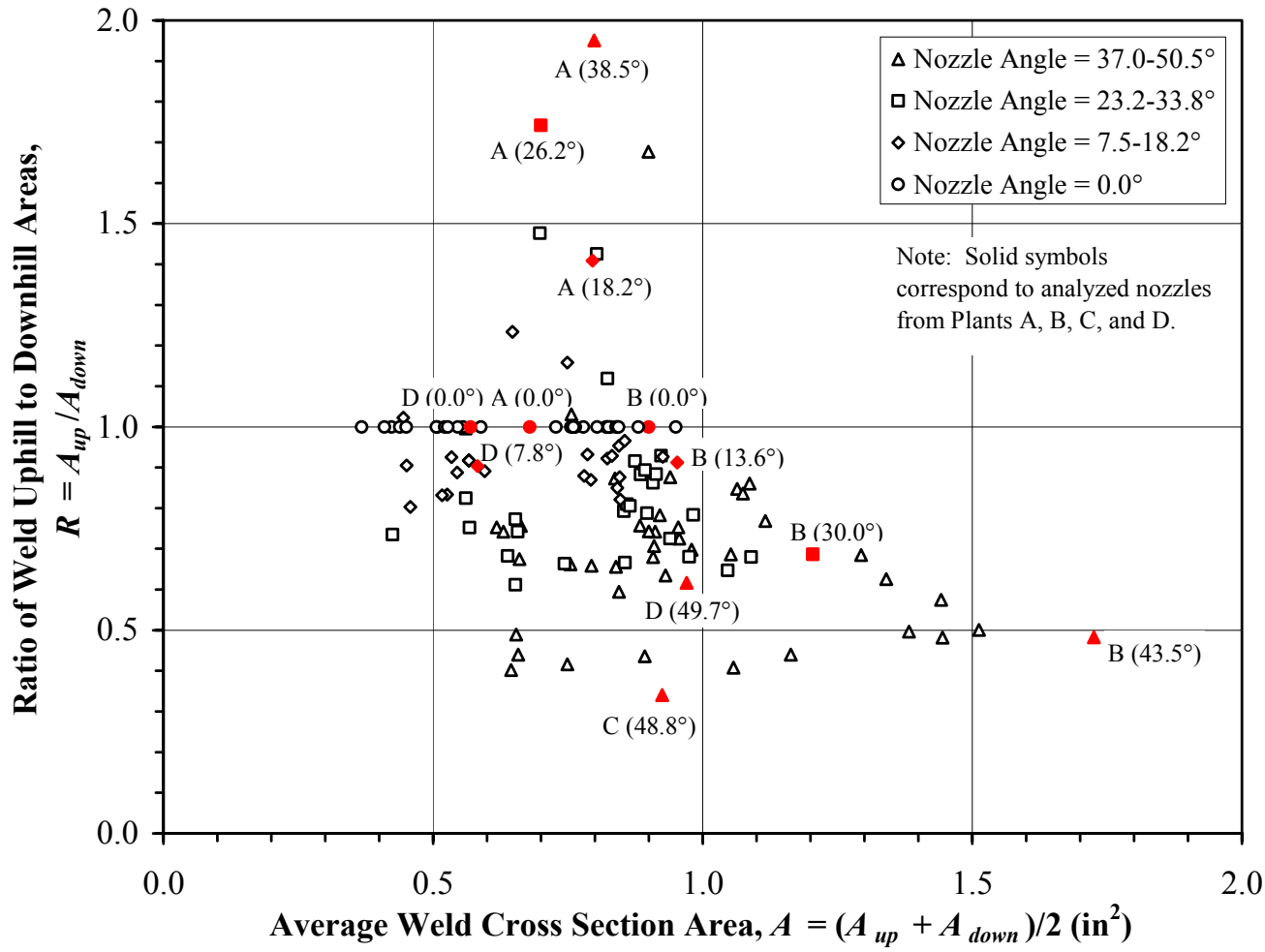

Figure 2-2
Comparison of Key Weld Geometry Variables Influencing Nozzle Residual Stresses – Plants Evaluated in this Study are Labeled

3
EXAMINATION ZONES

On the basis of the stress plots in Appendix A, an examination zone for volumetric examination of RPV top head nozzles has been defined as illustrated in Figure 3-1. The criteria used to establish this examination zone is that the examination zone will encompass all portions of the nozzle for which surface operating and residual stresses during normal plant operation exceed 20 ksi tension. As illustrated in Figure 3-1a), the examination zone for large nozzle angles with respect to the head (> 30°) includes the portion of the nozzles from one inch above the highest point of the root of the J-groove weld (on a horizontal plane perpendicular to the nozzle axis) to one inch below the lowest point at the toe of the J-groove weld on a horizontal plane perpendicular to the nozzle axis. For smaller angle nozzles with respect to the head (≤ 30°) and ICI nozzles, the inspection zone includes the portion of the nozzles from 1.5 inches above the highest point of the root of the J-groove weld (on a horizontal plane perpendicular to the nozzle axis) to 1.5 inches below the lowest point at the toe of the J-groove weld on a horizontal plane perpendicular to the nozzle axis (Fig. 3-1b). In nozzles for which the inspection zone dimensions in Figure 3-1 extend below the bottom end of the nozzle, the requirement is to inspect to the bottom of the nozzle.

Summaries of the stresses determined from the plots of Appendix A at the upper and lower boundaries of the examination zone are provided in Table 3-1 for the above-weld inspection zone and in Table 3-2 for the below-weld inspection zone. It is seen from these tables that the stresses at the edges of the inspection zone meet the 20 ksi tension limit by a large margin, with the exception of two cells which are shown shaded in the in the tables. A tensile stress of 20.2 ksi is reported on the ID surface, hoop direction, on the downhill side of the ICI nozzle above the weld in Table 3-1, and a tensile stress of 20.3 ksi is reported for the ID surface, axial direction, downhill side of the 8° CEDM nozzle below the weld in Table 3-2. These stress levels are highly localized, and are considered close enough to the 20 ksi limit to be considered acceptable. Additional margin is provided by the fracture mechanics calculations of Section 4.

Table 3-1
Evaluation of Stresses at Top Edge of Above-Weld Inspection Zone in Characteristic Plants

Plant	Nozzle Angle-Azimuth	Inspection Zone Dist. from Weld (inches)	Stresses at Edge of Inspection Zone Above Weld (ksi)			
			ID-Hoop	OD-Hoop	ID-Axial	OD-Axial
A	38-Downhill	5.65	8	1.4	1.8	3.1
	38-Sidehill	3.29	-3.1	-1.3	1.0	-0.1
	38-Uphill	1.00	14.2	-20.1	4.2	-7.6
A	26-Downhill	4.39	6.9	3.6	2.0	3.8
	26-Sidehill	2.93	0.0	3.1	2.3	3.7
	26-Uphill	1.50	5.4	-5.8	1.7	0.0
A	18-Downhill	3.37	4.6	0.4	4.2	1.2
	18-Sidehill	2.43	1.7	-0.2	5.5	0.1
	18-Uphill	1.50	3.9	-2.7	4.7	-2.3
A	0-All	1.50	7.0	-1.6	12.3	-7.8
B	43-Downhill	4.66	8.1	1.2	2.9	9.6
	43-Sidehill	2.80	1.1	0.6	-2.1	-4.8
	43-Uphill	1.00	15.8	-14.3	4.6	-7.0
B	30-Downhill	3.75	6.3	0.9	3.4	5.7
	30-Sidehill	2.62	2.5	2.4	-0.2	-1.3
	30-Uphill	1.50	1.3	-4.0	1.0	-3.6
B	13-Downhill	2.47	1.4	-1.4	7.7	1.6
	13-Sidehill	1.98	1.7	-1.9	7.4	-4.6
	13-Uphill	1.50	1.3	-4.4	6.3	-4.7
B	0-All	1.50	6.8	-3.9	14.4	-10.3
C	48-Downhill	5.15	13.7	-2.4	10.9	13.6
	48-Sidehill	3.04	-2.5	7.2	-1.0	0.4
	48-Uphill	1.00	11.5	-6.5	2.3	-7.4
D	49-Downhill	6.31	11.1	0.3	2.0	4.5
	49-Sidehill	3.59	-1.7	2.6	-2.1	1.3
	49-Uphill	1.00	15.5	-23.3	4.5	-12.4
D	8-Downhill	2.11	4.3	-2.0	10.6	-6.7
	8-Sidehill	1.81	4.1	-2.2	10.6	-6.3
	8-Uphill	1.50	6.0	-0.7	10.7	-7.3
D	55-Downhill(ICI)	9.88	20.2	1.7	2.2	4.6
	55-Sidehill(ICI)	5.51	5.4	13.9	-2.2	5.2
	55-Uphill(ICI)	1.50	19.1	-3.5	-1.9	-3.2

Table 3-2
Evaluation of Stresses at Bottom Edge of Below-Weld Inspection Zone in Characteristic Plants

Plant	Nozzle Angle-Azimuth	Inspection Zone Dist. from Weld (inches)	Stresses at Edge of Inspection Zone Above Weld (ksi)			
			ID-Hoop	OD-Hoop	ID-Axial	OD-Axial
A	38-Downhill	1.00	-24.9	-13.2	-1.5	0.2
	38-Sidehill	3.07	9.5	-7.9	4.4	-9.5
	38-Uphill	5.08	-16.0	-0.2	-1.3	-0.9
A	26-Downhill	1.50	-31.0	-20.5	1.8	-3.5
	26-Sidehill	2.77	-4.9	-9.9	4.8	-9.5
	26-Uphill	4.02	-10.8	-5.6	0.6	-5.2
A	18-Downhill	1.50	-25.1	-19.8	5.8	-7.6
	18-Sidehill	2.34	-13.5	-14.0	8.1	-11.7
	18-Uphill	3.18	-12.3	-11.8	5.4	-9.9
A	0-All	1.50	-23.0	-28.4	6.8	-11.0
B	43-Downhill	1.00	5.5	13.1	20.0	-18.5
	43-Sidehill	2.62	8.3	-12.3	17.2	-21.2
	43-Uphill	4.19	-14.6	-2.2	1.0	-1.3
B	30-Downhill	1.50	-8.4	-10.6	15.7	-15.5
	30-Sidehill	2.42	-1.9	-11.9	13.2	-15.7
	30-Uphill	3.32	-10.4	-6.4	2.9	-7.3
B	13-Downhill	1.50	-0.1	-13.1	18.8	-20.5
	13-Sidehill	1.78	-10.3	-14.3	18.2	-19.7
	13-Uphill	2.07	-10.1	-17.2	14.2	-17.2
B	0-All	1.50	-27.8	-33.2	8.1	-12.4
C	48-Downhill	1.00	-8.9	9.0	14.9	-7.8
	48-Sidehill	3.30	12.6	-12.4	9.9	-18.9
	48-Uphill	5.52	-12.1	-0.9	2.7	1.5
D	49-Downhill	1.00	2.3	7.5	15.8	-5.4
	49-Sidehill	3.55	4.2	-9.8	9.1	-18.1
	49-Uphill	5.99	-10.8	-0.4	-0.2	3.2
D	8-Downhill	1.50	6.3	-4.4	20.3	-20.6
	8-Sidehill	1.82	2.3	-7.7	18.6	-19.8
	8-Uphill	2.13	-1.4	-10.4	16.2	-17.9
D	55-Downhill(ICI)	1.50	N/A*	N/A*	N/A*	N/A*
	55-Sidehill(ICI)	5.48	N/A*	N/A*	N/A*	N/A*
	55-Uphill(ICI)	9.58	N/A*	N/A*	N/A*	N/A*

* - Inspection zone extends beyond the bottom edge of the nozzle.

a) Inspection zone for nozzle angles greater than 30°

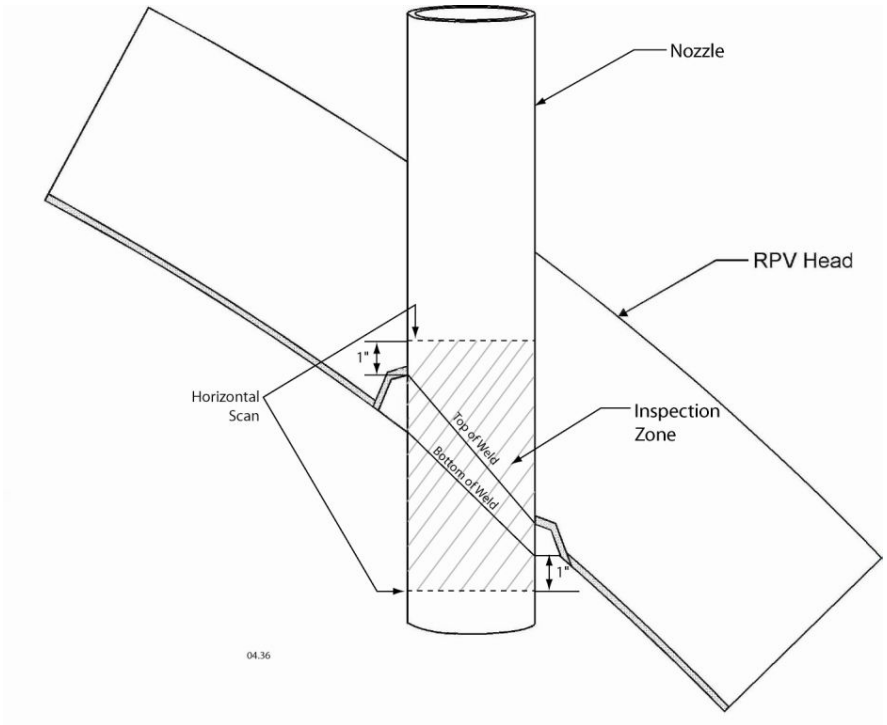

b) Inspection zone for nozzle angles less than or equal to 30° and ICI nozzles

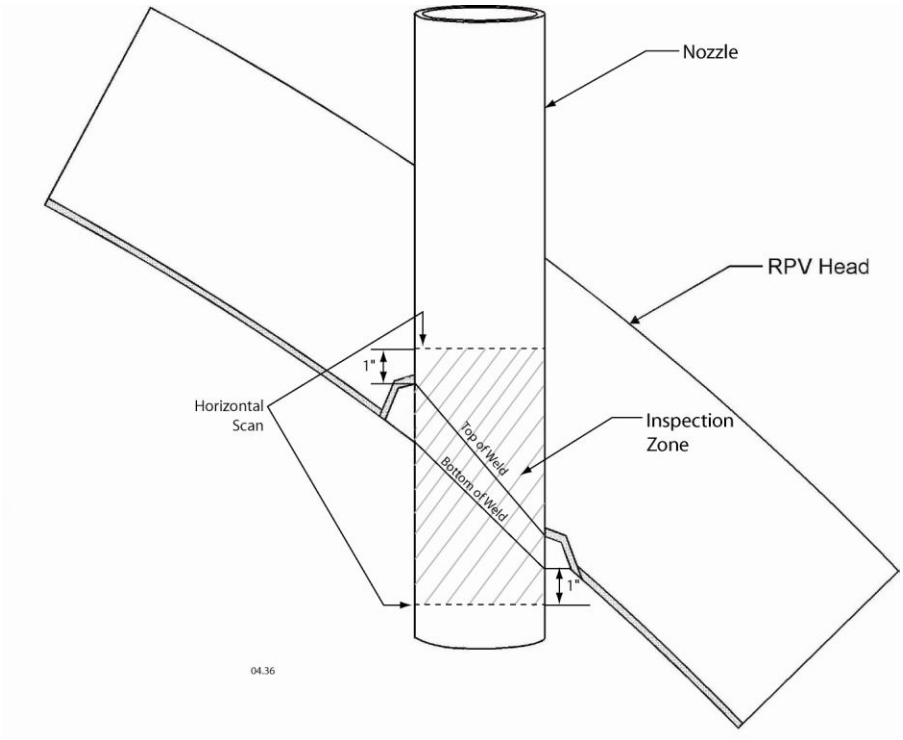

Figure 3-1
Illustration of RPV Top Head Nozzle Inspection Zone

4
FRACTURE MECHANICS ANALYSES

As further confirmation that the inspection zones defined in Section 3 provide an acceptable level of quality and safety, fracture mechanics calculations have also been performed to demonstrate that flaws which could potentially be missed because they are outside of the inspection zone would not grow to unacceptable sizes during the period of plant operation until the next scheduled volumetric or surface examination. Calculations are performed for axially oriented flaws in the nozzle end just below the inspection zone (Figure 4-1), as well as for circumferential flaws just above the inspection zone (Figure 4-2). The inspection requirements of Ref. [2] impose a maximum inspection interval of 3.0 RIYs, which are equivalent to 3.0 years of a plant operating at a top head temperature of 600°F. Crack growth evaluations are thus performed at this temperature for all of the characteristic plant types to demonstrate that the maximum size flaws that could potentially escape detection because they are outside the examination zone would not grow unacceptably in 3.0 years of full power operation.

4.1 Growth of Axial Cracks Below the Weld

The portions of the CRDM/CEDM tubes that extend into the reactor vessel below the J-groove welds are exposed to reactor water chemistry, and is thus potentially susceptible to PWSCC. The stresses that would drive such cracking are expected to be much lower than in the vicinity of the annulus or J groove weld, however, since internal and external pressure is the same, and since this portion of the tube that is outside of the inspection zone defined in Section 3 is, for the most part, remote from the high residual stresses associated with the J-groove weld. Assuming an examination zone as proposed in Section 3, the limiting flaw that could remain undetected in the portion of the tube below the J-groove weld is postulated to be a through-wall axial flaw propagating from the bottom of the tube upward to the lower edge of the examination zone (see Figure 4-1). If such a flaw were to grow to the bottom of the J-groove weld, it could potentially lead to leakage in a short period, since crack propagation rates in the weld metal are faster than in the Alloy-600 base metal, and the residual stresses in the weld are very high.

To demonstrate that the proposed inspection zones provide adequate protection against leakage, a series of deterministic fracture mechanics calculations were performed. The postulated initial flaw lengths are different for different plant types and locations, as listed in Table 4-1. Analyses were done for the downhill, sidehill, and uphill locations for various nozzle angles for each of the characteristic plant types. Analysis details are contained in Ref. [9].

Table 4-1
Starting Flaw Lengths for Crack Growth Analysis of Postulated Axial Cracks below J-Groove Welds

PLANT/NOZZLE	LOCATION	LENGTH (in. from bottom of nozzle to weld)	INSPECTION ZONE (in. below weld)	STARTING FLAW SIZE (in.)
Plant A				
(B&W 38°)	DOWNHILL	1.053	1.0	0.053
	SIDEHILL	3.122	3.069	0.053
	UPHILL	5.132	5.079	0.053
(B&W 0º)	ALL	1.624	1.5	0.124
Plant B				
(W 2-LOOP 43.5°)	DOWNHILL	1.917	1.0	0.917
	SIDEHILL	3.537	2.62	0.917
	UPHILL	5.104	4.187	0.917
(W 2-LOOP 30º)	DOWNHILL	1.953	1.5	0.453
	SIDEHILL	2.871	2.418	0.453
	UPHILL	3.775	3.332	0.453
(W 2-LOOP 13º)	DOWNHILL	1.967	1.5	0.467
	SIDEHILL	2.251	1.784	0.467
	UPHILL	2.534	2.067	0.467
(W 2-LOOP 0º)	ALL	1.632	1.5	0.132
Plant C				
(W 4-LOOP 48.8°)	DOWNHILL	2.134	1.0	1.134
	SIDEHILL	4.437	3.303	1.134
	UPHILL	6.650	5.516	1.134
Plant D				
(CE 49.7°)	DOWNHILL	2.498	1.0	1.498
	SIDEHILL	5.050	3.552	1.498
	UPHILL	7.490	5.992	1.498
(CE 8º)	DOWNHILL	2.558	1.5	1.058
	SIDEHILL	2.874	1.816	1.058
	UPHILL	3.189	2.131	1.058

Stresses for these analyses are taken from the stress distributions described in Section 2, and compiled in Appendix A. Specifically, hoop stress distributions (which would tend to open axial flaws in the tubes) were selected for the inside and outside surface of each nozzle for each azimuth (uphill, sidehill and downhill). These stresses include weld residual stresses, pressure stresses, and any other sustained applied loads affecting the hoop direction.

For conservatism and ease of calculation, the hypothetical axial cracks were modeled for fracture mechanics analyses as edge-connected through-wall cracks in a wide flat plate. This model does not account for the hoop constraint of the actual geometry, and therefore is conservative compared to the actual geometry.

In some cases, a portion of the axially oriented flaw resides in a compressive zone. In these cases, the compressive portion of the stress field was set to zero, so the flaw was only acted upon by tensile stresses.

The stress results were input to the SI fracture mechanics program **pc-CRACK** [10] to calculate the applied stress intensity factor ($K_{applied}$) distribution for each case. K was determined for crack lengths spanning the complete length of each tube, from the bottom-most edge, to the start of the J-Groove weld. K was determined as a function of distance from the bottom edge of the tube, for each plant type, for the downhill, sidehill, and uphill flaw locations.

Flaw growth rate correlations were determined for these assumed flaw locations as a function of temperature, using the methods of MRP-55 [11]. This results in a crack growth correlation of

$$da/dt = A\,(K_{applied}-K_{threshhold})^{1.16} \text{ inch/hour}$$

where:

A = Crack growth coefficient (2.77×10^{-7} at 600°F)

$K_{applied}$= the K distribution as determined above

$K_{threshhold}$= 8.19 ksi-√in

Crack growth calculations were performed for the assumed initial flaw sizes listed in Table 4-1, using the K distributions and this crack growth correlation. Results are summarized in Table 4-2. This table shows that, for all but three of the cases studied, the applied K at the assumed initial flaw size (just impinging on the inspection zone) does not exceed the threshold stress intensity factor value, and consequently for these cases, no flaw growth is predicted. In one case (W 4-loop, 48.8° nozzle), the initial applied K is above the threshold value (allowing growth) but the applied K drops below the threshold after a short period of growth, so the initial flaw is predicted to arrest before reaching the weld. In the remaining two cases, continuing growth is predicted, and the growth time required to reach the J groove weld is included in the table. The minimum crack growth time reported in Table 4-2 is 135,000 hours, which corresponds to over fifteen years of plant operation (EFPYs) at a 600°F operating temperature. This is clearly greater than the 3.0 RIY inspection interval imposed in Reference [2].

The below-weld inspection zones in Figure 3-1 are thus shown to be acceptable by fracture mechanics crack growth calculations. Even if a small flaw were to exist in the uninspected portions of the nozzles at the time of inspection (which is highly unlikely, since the stresses there are below 20 ksi tension), conservative crack growth calculations show that it would not propagate through the inspection zone to the weld, and thus potentially lead to leakage before the next required inspection.

Table 4-2
Crack Growth Times for Postulated Axial Cracks at Edge of Below Weld Inspection Zone to Reach Weld (Minimum Time is Greater than Fifteen EFPYs)

PLANT/ NOZZLE	LOCATION	K @ STARTING FLAW SIZE (KSI-√IN)	CRACK GROWTH TIME TO BOTTOM OF J-GROOVE WELD (HOURS) @600˚F
Plant A			
(B&W 38°)	DOWNHILL	< 8.19	No Growth
	SIDEHILL	< 8.19	No Growth
	UPHILL	< 8.19	No Growth
(B&W 0°)	ALL	< 8.19	No Growth
Plant B			
(W 2-LOOP 43.5°)	DOWNHILL	< 8.19	No Growth
	SIDEHILL	21.8	135000
	UPHILL	< 8.19	No Growth
(W 2-LOOP 30°)	DOWNHILL	< 8.19	No Growth
	SIDEHILL	< 8.19	No Growth
	UPHILL	< 8.19	No Growth
(W 2-LOOP 13°)	DOWNHILL	< 8.19	No Growth
	SIDEHILL	< 8.19	No Growth
	UPHILL	< 8.19	No Growth
(W 2-LOOP 0°)	ALL	< 8.19	No Growth
Plant C			
(W 4-LOOP 48.8°)	DOWNHILL	< 8.19	No Growth
	SIDEHILL	< 8.19	No Growth
	UPHILL	37.7	Arrests
Plant D			
(CE 49.7°)	DOWNHILL	< 8.19	No Growth
	SIDEHILL	32.4	182000
	UPHILL	< 8.19	No Growth
(CE 8°)	DOWNHILL	< 8.19	No Growth
	SIDEHILL	< 8.19	No Growth
	UPHILL	< 8.19	No Growth

4.2 Growth of Circumferential Cracks Above the Weld

Crack growth correlations for the annulus region above the weld were also developed using the crack growth correlation recommended in MRP-55 [11] for a 600°F head operating temperature. These crack growth analyses were again performed with the SI program **pc-CRACK** [10] to determine the predicted crack growth for initial through-wall circumferential flaws assumed to exist at the top edge of the above-weld inspection zone. As illustrated in Figure 4-2, initial flaw lengths equal to 30° of the nozzle circumference were assumed, centered at both the uphill and downhill azimuths. Justification for this assumed initial flaw size is based on the fact that the nozzles will also have been inspected for leakage, prior to or in conjunction with this NDE. If leakage was detected, the nozzle will be repaired or replaced. IF no leakage is detected, there is strong expectation that no circumferential cracks exist, and in this case, assumption of a 30° of circumference, circumferential crack has been shown to be conservative [12].

Previous analyses reported in [12] developed stress intensity factor results for postulated circumferentially oriented cracks in the critical (steepest angle) nozzles of the four characteristic plant types. The results were developed using finite element analysis methods, parametrically varying flaw lengths to determine stress intensity factor versus flaw length. The results are summarized for the four characteristic plant types in Tables 4-3, 4-4, 4-5, and 4-6.

These stress intensity factor results are based on an envelope stress distribution of bounding axial residual and applied stresses above the weld, for the limiting (highest angle) nozzles. The envelope stresses are shown in Figure 4-3, compared to axial stresses above the weld at the inspection zone boundary for the steepest angle and smaller angle nozzles. The envelope stresses assumed clearly bound the applied stresses at the edge of the examination zone.

The stress intensity factor results in Tables 4-3, 4-4, 4-5, and 4-6 were used to compute the growth of the assumed circumferential through-wall flaws from 30° of circumference to a length of 300°. Analysis details are contained in Reference [13]. 300° corresponds generally to the greatest flaw length that maintains the factors of safety contained in ASME Section XI, IWB-3600 against nozzle ejection. An above-weld flaw growth correlation for the assumed 600°F top head temperature was used [11], which incorporates a factor of 2 increase over that discussed above in Section 4.1, to account for potentially severe chemistry conditions in the annulus between the nozzle and the reactor vessel head. In these analyses, because the assumed flaw is double ended, growth is assumed to occur simultaneously from both crack tips. Growth is thus determined for a half-length flaw to a half-allowable size, using the calculated K vs. a data and the temperature dependent PWSCC crack growth correlations. The resulting initial and final flaw size and growth time is equivalent to a flaw growing at both ends.

Table 4-3
Stress Intensity Factor for Above-Weld Circumferential Flaws for Plant A (B&W Type Plant - 38° Nozzle - Envelop Stress Distributions)

Total Flaw Angle (Degrees)	Stress Intensity Factors, K (psi-√in)	
	Downhill	*Uphill*
30	11227	20141
90	33760	37722
160	68230	51559
180	78168	54337
220	94384	56867
260	115569	59702
300	140472	64773

Table 4-4
Stress Intensity Factor for Above-Weld Circumferential Flaws for Plant B (W 2-Loop Plant - 43.5º Nozzle - Envelop Stress Distributions)

Total Flaw Angle (Degrees)	Stress Intensity Factors, K (psi-√in)	
	Downhill	*Uphill*
30	20599	10791
180	79528	26475
220	95130	26392
260	108876	31101
300	113957	40949

Table 4-5
Stress Intensity Factor for Above-Weld Circumferential Flaws for Plant C (W 4-Loop Plant – 48.8º Nozzle - Envelop Stress Distributions)

Total Flaw Angle (Degrees)	Stress Intensity Factors, K (psi-√in)	
	Downhill	*Uphill*
30	28790	4942
90	59336	14302
160	84080	21782
180	86557	24115
220	89310	30100
260	92769	38017
300	93453	50009

Table 4-6
Stress Intensity Factor for Above-Weld Circumferential Flaws for Plant D (CE Plant – 49.7º Nozzle - Envelop Stress Distributions)

Total Flaw Angle (Degrees)	Stress Intensity Factors, K (psi-√in)Average	
	Downhill	*Uphill*
30	16514	14873
180	62914	73987
220	71523	71713
260	82489	64444
300	98657	62413

Crack growth results are presented in Table 4-7 in terms of the time required to grow from the assumed initial flaw size (30°) to the allowable size (300°). The results in Table 4-7 are reported in units of both effective full power hours and effective full power years. (One EFPY equals 8760 EFPH.) The limiting result in Table 4-7 is the downhill side of Plant C - 48.8° nozzle, for which growth of an initial 30-degree crack to 300° is predicted to occur in 9.31 EFPY at 600ºF. The circumferential crack growth results are all significantly greater than the 3.0 RIY inspection interval imposed in Reference [2].

The above-weld inspection zones in Figure 3-1 are thus shown to be acceptable by fracture mechanics crack growth calculations. Even if a small flaw were to exist in the uninspected portions of the nozzles at the time of inspection (which is highly unlikely, since the stresses there are below 20 ksi tension), conservative crack growth calculations show that it would not propagate to an unacceptable size, and thus potentially lead to nozzle ejection before the next required inspection.

Table 4-7
Growth Time from 30° to 300° Circumferential Cracks in Limiting Nozzles in Four Characteristic Plants (Assumed top head temperature = 600°F)

PLANT - NOZZLE	UPHILL (EFPH)	UPHILL (EFPY)	DOWNHILL (EFPH)	DOWNHILL (EFPY)
Plant A - 38° Nozzle	154874	17.68	193501	22.09
Plant B - 43.5° Nozzle	521114	61.89	94970	10.84
Plant C – 48.8° Nozzle	no growth	no growth	81572	9.31
Plant D – 49.7° Nozzle	167465	19.12	164293	18.75

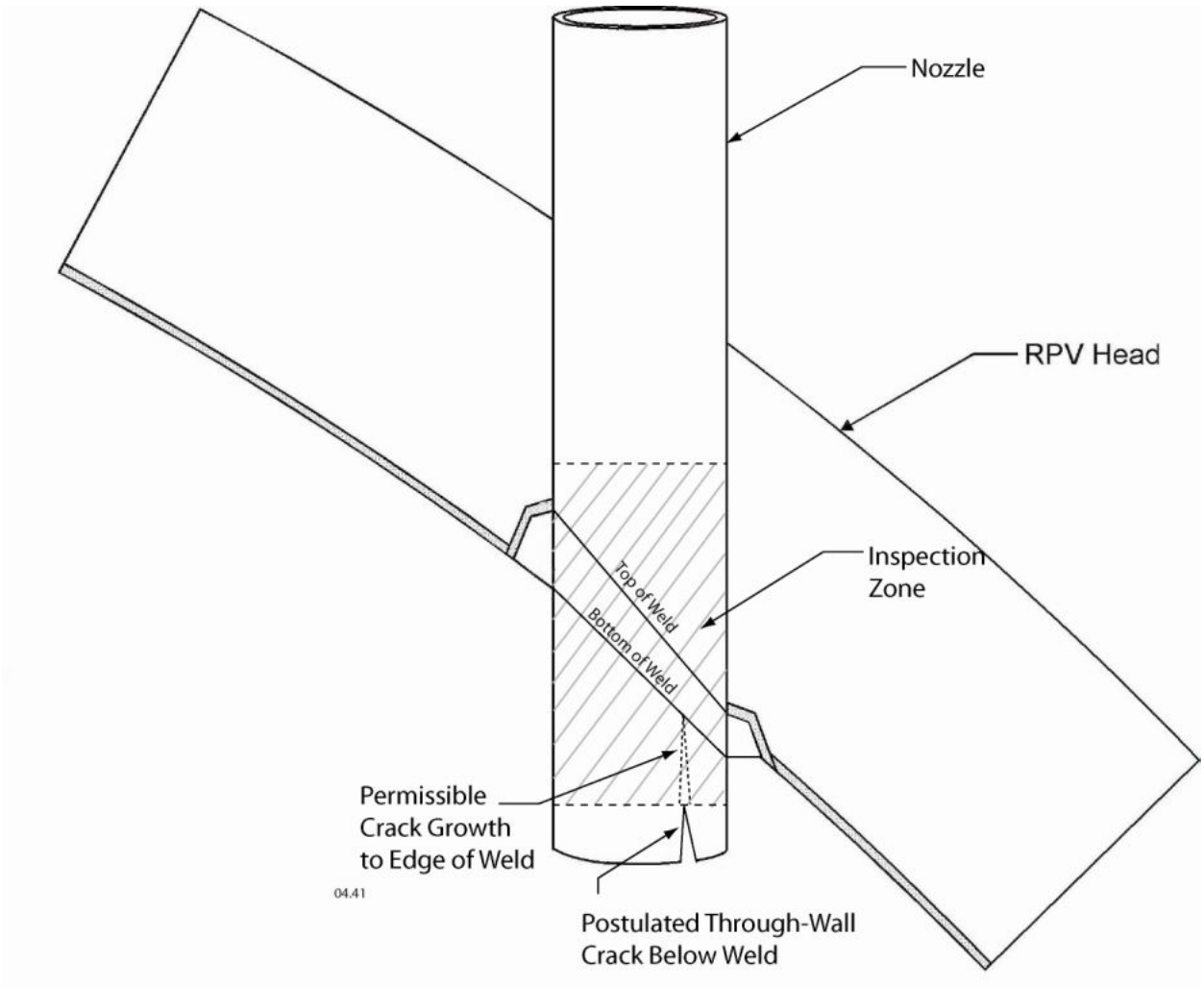

Figure 4-1
Illustration of Assumed Axial Flaw and Permissible Crack Growth Below the Weld Inspection Zone

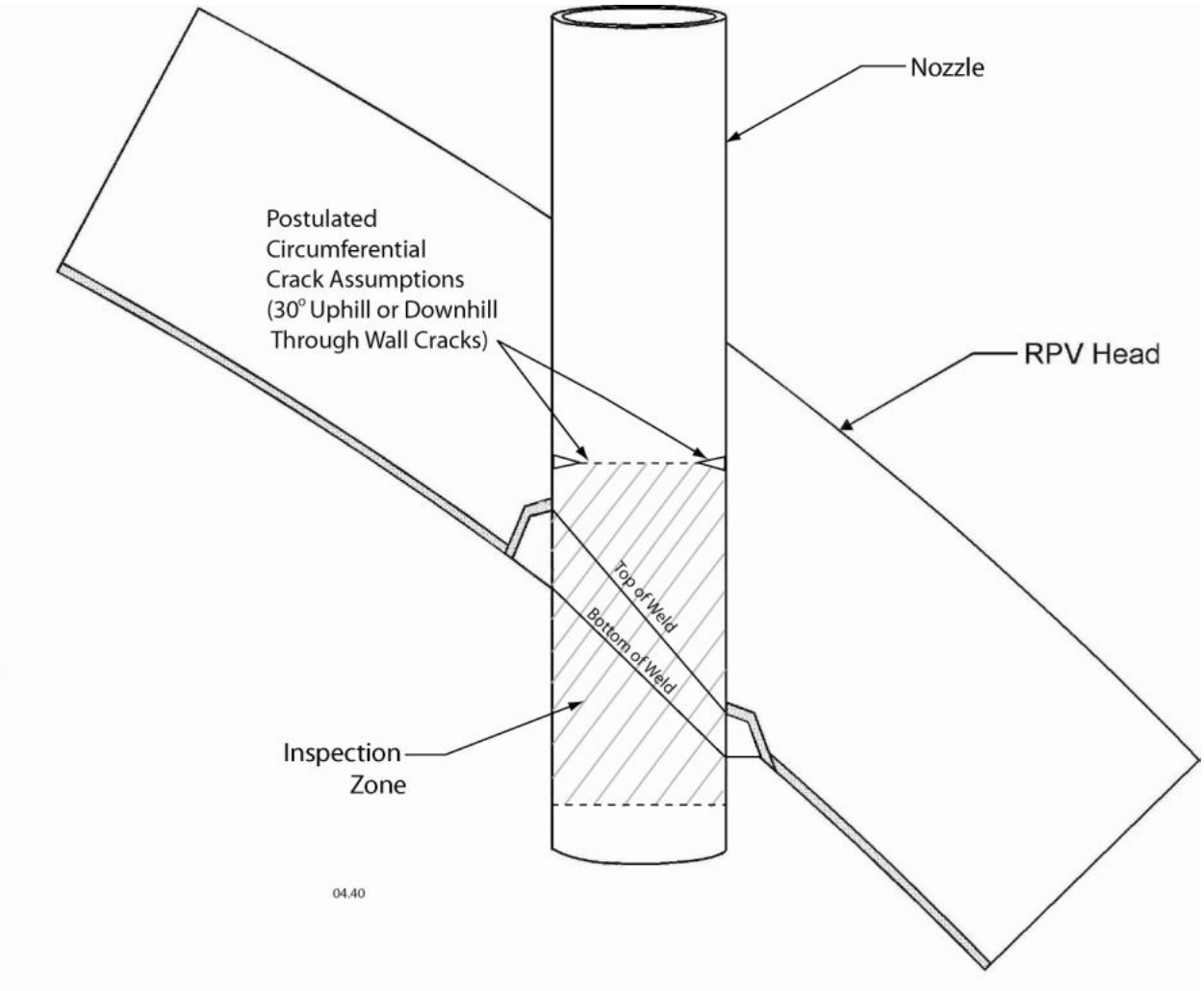

Figure 4-2
Illustration of Assumed Circumferential Flaws Above the Weld Inspection Zone

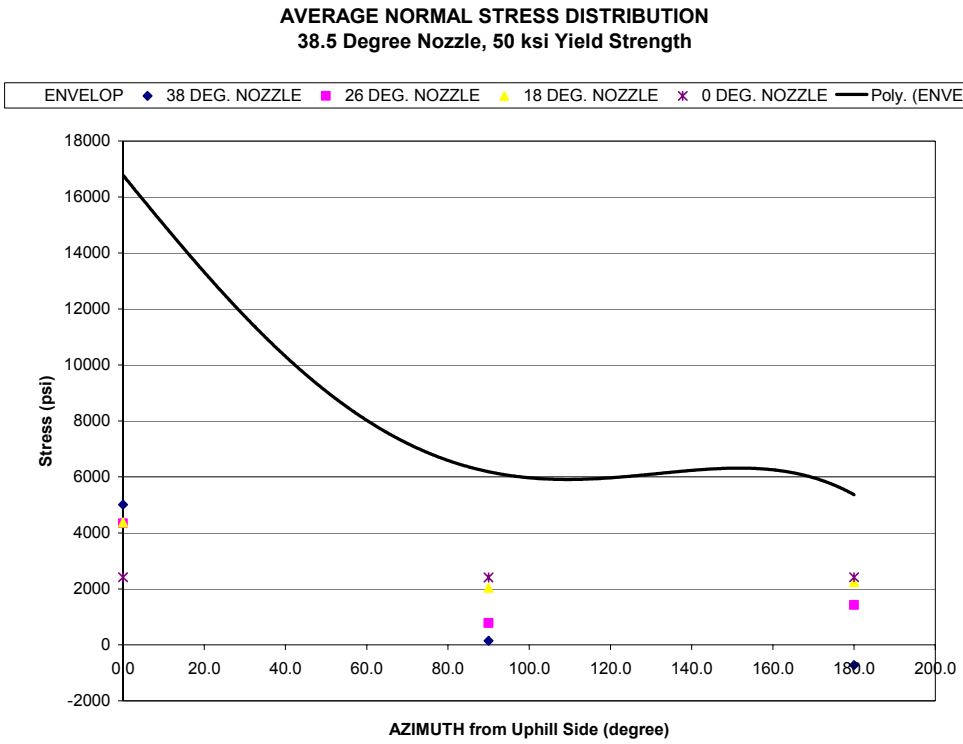

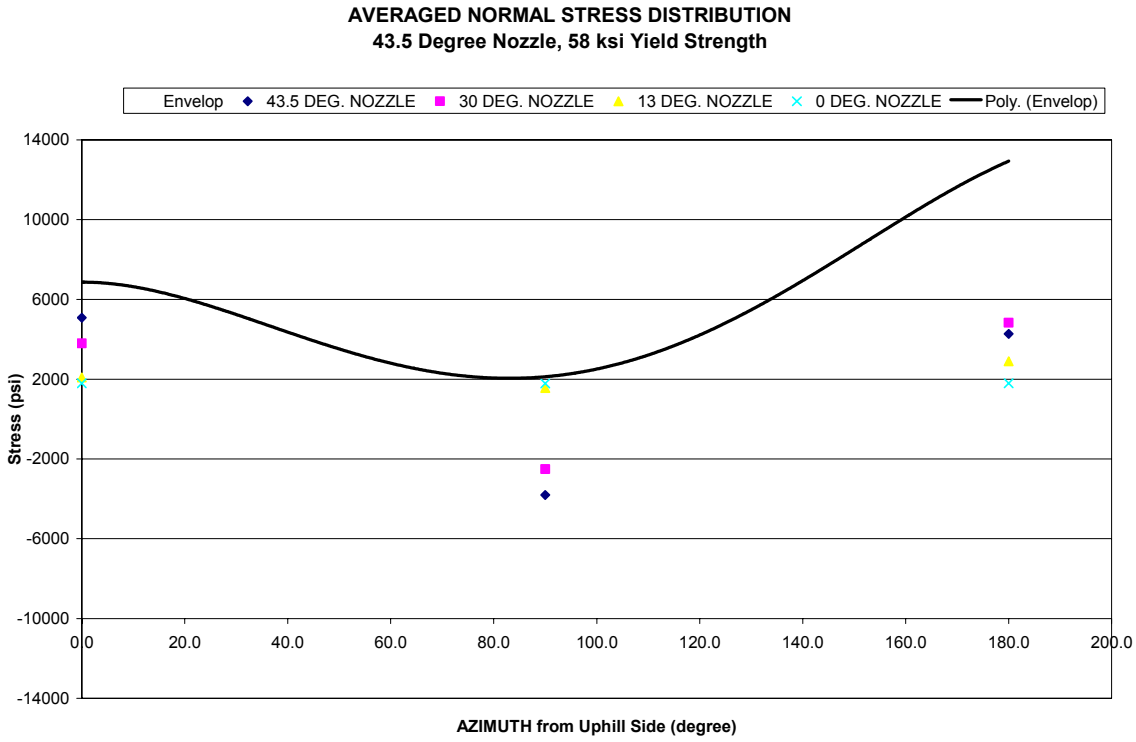

Figure 4-3
Envelope Stresses Compared to Stresses at Edge of Inspection Zone

5
COMPARISON TO PAST INSPECTION RESULTS

Finally, a review of past top head inspection results for U.S. PWRs was performed to determine if flaws were found in prior inspections that were completely outside of the new inspection zone definition, and would thus be missed if the revised inspection zones were implemented. Figure 5-1 presents a plot of the past inspection data for the CRDMs for several plants in the U.S.

It should be noted that weld height is not represented in the vertical axis; all distances on the vertical axis represent distances above the top and below the bottom of the weld. Therefore, flaws that begin (or end) anywhere within the weld are shown as beginning (or ending) at the zero-inch line. Similarly, flaws that are completely contained within the weld are shown as a point on the zero inch line.

The Figure 5-1 plot shows that of the 237 data points studied, 3 flaws (shown in green squares) begin at a distance greater than 1 inch above the weld and proceed away from the weld. Similarly, 22 flaws (shown in red circles) begin at a distance greater than 1 inch below the weld and proceed away from the weld. A portion of each of the remaining 212 flaws is within the 1-inch distance above or below the weld. To determine if the 25 flaws would be encompassed in the area between horizontal scans at 1 inch above the top of the weld on the uphill side and 1 inch below the bottom of the weld on the downhill side (horizontal scan region), azimuthal locations of these 25 flaws were examined further. It was found that a portion of all 25 flaws are within the recommended inspection zone.

Therefore, in the prior inspections dataset examined, all flaws were found to be within the new inspection zone definition, and would thus be detected if the revised inspection zones were implemented. This dataset represents a significant cross section of the CRDM/CEDM inspection findings in U.S. PWRs.

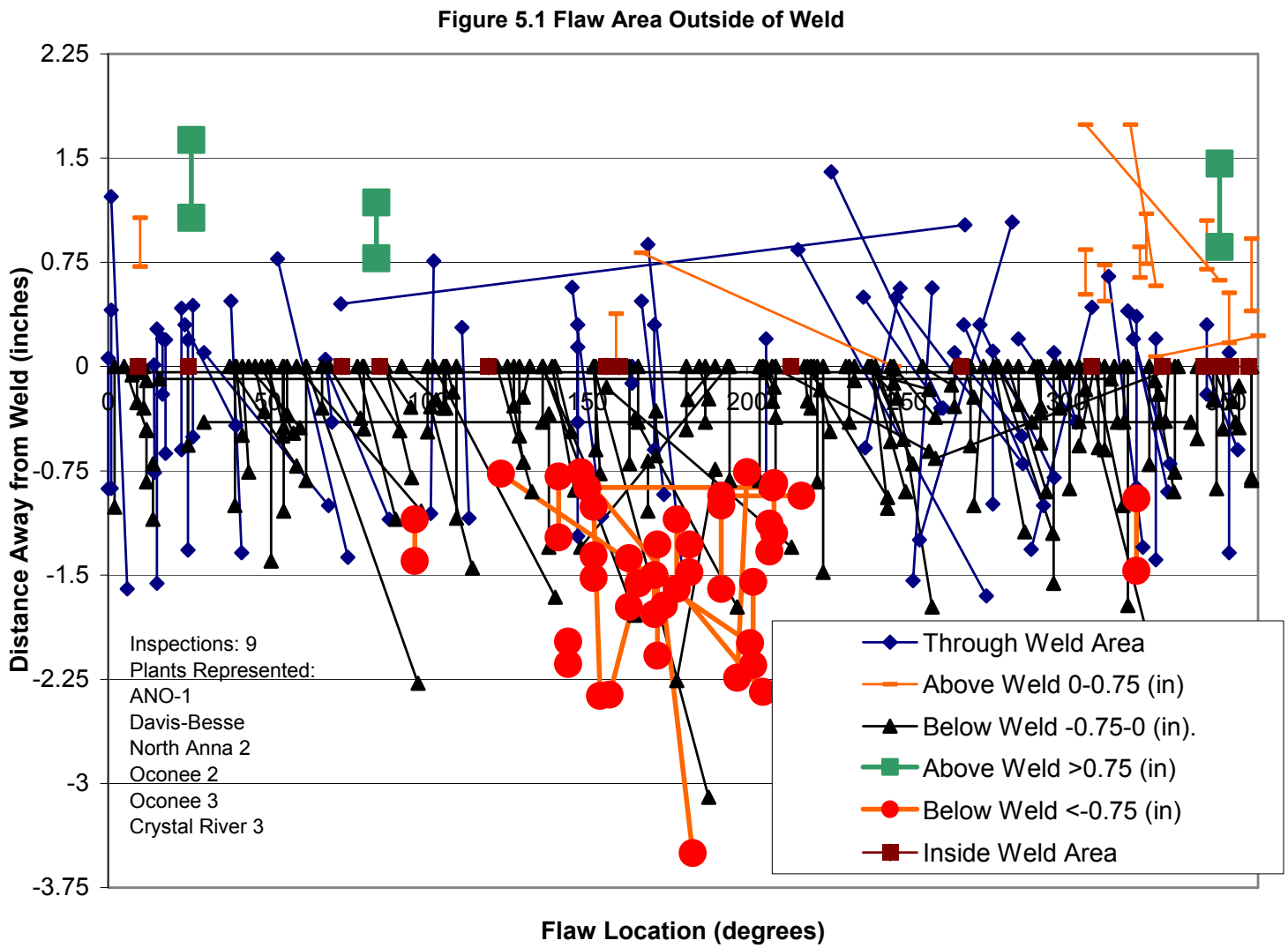

Figure 5-1
Flaw Area Outside of Weld

6
CONCLUSIONS

This report contains a generic technical evaluation to justify an examination zone for PWR top head inspections contained in the MRP top head inspection plan [2]. It addresses extent of examination both above the top and below the bottom of the J-groove weld. The evaluation considers stresses in a group of characteristic plants that bound the fleet of U.S. PWRs from the standpoint of the important factors that contribute to nozzle residual and operating stresses. Plots of stress versus distance above and below the J-groove weld are developed for several nozzles in these plants. An inspection zone is them defined, beyond which the stresses decay significantly, to levels at which primary water stress corrosion cracking (PWSCC) is considered highly unlikely. Then, assuming (non-mechanistically) that cracks form in the uninspected regions up to and impinging upon the proposed inspection zone, fracture mechanics calculations are performed to demonstrate that such cracks would not propagate to an unacceptable size in the time period until the next required inspections. Finally, NDE data are reviewed and presented to demonstrate the effectiveness of the proposed examination zones with respect to prior inspection results for U.S. PWR top head nozzles.

The results of this evaluation support an inspection zone illustrated schematically in Figure 3-1 of this report. The inspection zone corresponds to a right circular cylinder extending from 1 inch above the highest point of the root of the J-groove weld to 1 inch below the lowest point of the toe of the weld for large angle CRDM and CEDM nozzles (>30°). For smaller angle nozzles (≤30°) and ICI nozzles, the cylinder extends from 1.5 inches above the highest point of the root of the J-groove weld to 1.5 inches below the lowest point of the toe of the weld.

The report establishes a reasonable target stress value (20 ksi tension), below which the probability of PWSCC is extremely remote, and demonstrates that, in all but a few isolated cases, the inspection zone, as defined above, envelopes all locations with stresses above this stress level. In no case does the examination zone exclude locations with stresses higher than 20.3 ksi. The report also includes PWSCC growth calculations of postulated flaws that could be overlooked due to unexamined regions, to demonstrate that such flaws, either above or below the weld, would not grow to unacceptable sizes in the time period until the next inspection required by the inspection plan [2]. Finally, review of prior plant inspection data from a large cross-section of U.S. PWRs revealed that, of 237 flaw indications reported in these inspections, all flaws would have been detected had the inspections been limited to just the above examination zone.

7
REFERENCES

1.0 U.S. NRC Revised Order EA-03-009, "Interim Inspection Requirements for Reactor Pressure Vessel Heads at Pressurized Water Reactors", issued on February 20, 2003

2.0 MRP-117, "Materials Reliability Program Inspection Plan for Reactor Vessel Closure Head Penetrations in U.S. PWR Plants - MRP Inspection Requirements", EPRI Report 1007830, DRAFT Final Report, July 6, 2004

3.0 MRP-110, "Materials Reliability Program Reactor Vessel Closure Head Penetration Safety Assessment for U.S. PWR Plants - Evaluations Supporting the MRP Inspection Plan", EPRI Report. 1009807, Final Report, May 2004

4.0 K. M. Boursier et al (EDF), "Effect of Strain Rate on SCC in High Temperature Primary Water, Comparison between Alloys 690 and 600", ANS 11th Environmental Degradation Meeting, August, 2003

5.0 Dominion Engineering, Inc. Calculation No. C-4142-00-2, Rev. 0, "Plant A CRDM Stress Analysis," 8/29/01, (Proprietary)

6.0 Dominion Engineering, Inc. Calculation No. C-7612-00-1, Rev. 0, "Plant B CRDM Stress Analysis," October 31, 2001, (Proprietary)

7.0 Dominion Engineering, Inc. Calculation No. R-7613-00-1, Rev. 0, "Plant C Fall 2002 CRDM Repair Analysis", January 2003, (Proprietary)

8.0 Dominion Engineering, Inc. Calculation No. C-7736-00-8, Rev. 0, "Plant D CEDM and ICI Stress Analysis – Alternate Element Mesh", 03/08/02, (Proprietary)

9.0 Structural Integrity Associates Calculation EPRI-182Q-310, "Deterministic Fracture Mechanics Crack Growth Calculations – Axial Flaws below Weld", Rev. 1, July 20, 2004.

10.0 Structural Integrity Associates, pc-CRACK for Windows, version 3.1-98348

11.0 Materials Reliability Program (MRP), "Crack Growth Rates for Evaluating Primary Water Stress Corrosion Cracking (PWSCC) of Thick-Wall Alloy 600 Material", MRP-55, Revision 1, November 2002. EPRI Proprietary

12.0 MRP-105, "Probabilistic Fracture Mechanics Analysis of PWR Reactor Pressure Vessel Top Head Nozzle Cracking, EPRI Report 1007834, prepared by Structural Integrity Associates, Final Report, May 2004

13.0 Structural Integrity Associates Calculation EPRI-182Q-307, "Deterministic Fracture Mechanics Crack Growth Calculations – Circumferential Flaws above Weld", Sept. 5, 2003.

A
APPENDIX A

This appendix contains stress plots for the nozzles analyzed in the four characteristic plants. Plots include hoop and axial stresses for each nozzle for the uphill, sidehill and downhill azimuths

Content Deleted – MRP/EPRI Proprietary Material

Figure A-1
Plant A (B&W) 38º Nozzle downhill Hoop Stress

Content Deleted – MRP/EPRI Proprietary Material

Figure A-2
Plant A (B&W) 38º Nozzle downhill Axial Stress

Content Deleted – MRP/EPRI Proprietary Material

Figure A-3
Plant A (B&W) 38º Nozzle sidehill Hoop Stress

Content Deleted – MRP/EPRI Proprietary Material

Figure A-4
Plant A (B&W) 38º Nozzle sidehill Axial Stress

Content Deleted – MRP/EPRI Proprietary Material

Figure A-5
Plant A (B&W) 38º Nozzle uphill Hoop Stress

Content Deleted – MRP/EPRI Proprietary Material

Figure A-6
Plant A (B&W) 38º Nozzle uphill Axial Stress

Content Deleted – MRP/EPRI Proprietary Material

Figure A-7
Plant A (B&W) 26º Nozzle downhill Hoop Stress

Content Deleted – MRP/EPRI Proprietary Material

Figure A-8
Plant A (B&W) 26º Nozzle downhill Axial Stress

Content Deleted – MRP/EPRI Proprietary Material

Figure A-9
Plant A (B&W) 26º Nozzle sidehill Hoop Stress

Content Deleted – MRP/EPRI Proprietary Material

Figure A-10
Plant A (B&W) 26º Nozzle sidehill Axial Stress

Content Deleted – MRP/EPRI Proprietary Material

Figure A-11
Plant A (B&W) 26º Nozzle uphill Hoop Stress

Content Deleted – MRP/EPRI Proprietary Material

Figure A-12
Plant A (B&W) 26º Nozzle uphill Axial Stress

Content Deleted – MRP/EPRI Proprietary Material

Figure A-13
Plant A (B&W) 18º Nozzle downhill Hoop Stress

Content Deleted – MRP/EPRI Proprietary Material

Figure A-14
Plant A (B&W) 18º Nozzle downhill Axial Stress

Content Deleted – MRP/EPRI Proprietary Material

Figure A-15
Plant A (B&W) 18º Nozzle sidehill Hoop Stress

Content Deleted – MRP/EPRI Proprietary Material

Figure A-16
Plant A (B&W) 18º Nozzle sidehill Axial Stress

Content Deleted – MRP/EPRI Proprietary Material

Figure A-17
Plant A (B&W) 18º Nozzle uphill Hoop Stress

Content Deleted – MRP/EPRI Proprietary Material

Figure A-18
Plant A (B&W) 18º Nozzle uphill Axial Stress

Content Deleted – MRP/EPRI Proprietary Material

Figure A-19
Plant A (B&W) 0º Nozzle downhill Hoop Stress

Content Deleted – MRP/EPRI Proprietary Material

Figure A-20
Plant A (B&W) 0º Nozzle downhill Axial Stress

Content Deleted – MRP/EPRI Proprietary Material

Figure A-21
Plant A (B&W) 0º Nozzle sidehill Hoop Stress

Content Deleted – MRP/EPRI Proprietary Material

Figure A-22
Plant A (B&W) 0º Nozzle sidehill Axial Stress

Content Deleted – MRP/EPRI Proprietary Material

Figure A-23
Plant A (B&W) 0º Nozzle uphill Hoop Stress

Content Deleted – MRP/EPRI Proprietary Material

Figure A-24
Plant A (B&W) 0º Nozzle uphill Axial Stress

Content Deleted – MRP/EPRI Proprietary Material

Figure A-25
Plant B (Westinghouse 2-loop) 43º Nozzle downhill Hoop Stress

Content Deleted – MRP/EPRI Proprietary Material

Figure A-26
Plant B (Westinghouse 2-loop) 43º Nozzle downhill Axial Stress

Content Deleted – MRP/EPRI Proprietary Material

Figure A-27
Plant B (Westinghouse 2-loop) 43º Nozzle sidehill Hoop Stress

Content Deleted – MRP/EPRI Proprietary Material

Figure A-28
Plant B (Westinghouse 2-loop) 43º Nozzle sidehill Axial Stress

Content Deleted – MRP/EPRI Proprietary Material

Figure A-29
Plant B (Westinghouse 2-loop) 43º Nozzle uphill Hoop Stress

Content Deleted – MRP/EPRI Proprietary Material

Figure A-30
Plant B (Westinghouse 2-loop) 43º Nozzle uphill Axial Stress

Content Deleted – MRP/EPRI Proprietary Material

Figure A-31
Plant B (Westinghouse 2-loop) 30º Nozzle downhill Hoop Stress

Content Deleted – MRP/EPRI Proprietary Material

Figure A-32
Plant B (Westinghouse 2-loop) 30º Nozzle downhill Axial Stress

Content Deleted – MRP/EPRI Proprietary Material

Figure A-33
Plant B (Westinghouse 2-loop) 30º Nozzle sidehill Hoop Stress

Content Deleted – MRP/EPRI Proprietary Material

Figure A-34
Plant B (Westinghouse 2-loop) 30º Nozzle sidehill Axial Stress

Content Deleted – MRP/EPRI Proprietary Material

Figure A-35
Plant B (Westinghouse 2-loop) 30º Nozzle uphill Hoop Stress

Content Deleted – MRP/EPRI Proprietary Material

Figure A-36
Plant B (Westinghouse 2-loop) 30º Nozzle uphill Axial Stress

Content Deleted – MRP/EPRI Proprietary Material

Figure A-37
Plant B (Westinghouse 2-loop) 13º Nozzle downhill Hoop Stress

Content Deleted – MRP/EPRI Proprietary Material

Figure A-38
Plant B (Westinghouse 2-loop) 13º Nozzle downhill Axial Stress

Content Deleted – MRP/EPRI Proprietary Material

Figure A-39
Plant B (Westinghouse 2-loop) 13º Nozzle sidehill Hoop Stress

Content Deleted – MRP/EPRI Proprietary Material

Figure A-40
Plant B (Westinghouse 2-loop) 13º Nozzle sidehill Axial Stress

Content Deleted – MRP/EPRI Proprietary Material

Figure A-41
Plant B (Westinghouse 2-loop) 13º Nozzle uphill Hoop Stress

Content Deleted – MRP/EPRI Proprietary Material

Figure A-42
Plant B (Westinghouse 2-loop) 13º Nozzle uphill Axial Stress

Content Deleted – MRP/EPRI Proprietary Material

Figure A-43
Plant B (Westinghouse 2-loop) 0º Nozzle downhill Hoop Stress

Content Deleted – MRP/EPRI Proprietary Material

Figure A-44
Plant B (Westinghouse 2-loop) 0º Nozzle downhill Axial Stress

Content Deleted – MRP/EPRI Proprietary Material

Figure A-45
Plant B (Westinghouse 2-loop) 0º Nozzle sidehill Hoop Stress

Content Deleted – MRP/EPRI Proprietary Material

Figure A-46
Plant B (Westinghouse 2-loop) 0º Nozzle sidehill Axial Stress

Content Deleted – MRP/EPRI Proprietary Material

Figure A-47
Plant B (Westinghouse 2-loop) 0º Nozzle uphill Hoop Stress

Content Deleted – MRP/EPRI Proprietary Material

Figure A-48
Plant B (Westinghouse 2-loop) 0º Nozzle uphill Axial Stress

Content Deleted – MRP/EPRI Proprietary Material

Figure A-49
Plant C (Westinghouse 4-loop) 48º Nozzle downhill Hoop Stress

Content Deleted – MRP/EPRI Proprietary Material

Figure A-50
Plant C (Westinghouse 4-loop) 48º Nozzle downhill Axial Stress

Content Deleted – MRP/EPRI Proprietary Material

Figure A-51
Plant C (Westinghouse 4-loop) 48º Nozzle sidehill Hoop Stress

Content Deleted – MRP/EPRI Proprietary Material

Figure A-52
Plant C (Westinghouse 4-loop) 48º Nozzle sidehill Axial Stress

Content Deleted – MRP/EPRI Proprietary Material

Figure A-53
Plant C (Westinghouse 4-loop) 48º Nozzle uphill Hoop Stress

Content Deleted – MRP/EPRI Proprietary Material

Figure A-54
Plant C (Westinghouse 4-loop) 48º Nozzle uphill Axial Stress

Content Deleted – MRP/EPRI Proprietary Material

Figure A-55
Plant D (CE) 49º Nozzle downhill Hoop Stress

Content Deleted – MRP/EPRI Proprietary Material

Figure A-56
Plant D (CE) 49º Nozzle downhill Axial Stress

Content Deleted – MRP/EPRI Proprietary Material

Figure A-57
Plant D (CE) 49º Nozzle sidehill Hoop Stress

Content Deleted – MRP/EPRI Proprietary Material

Figure A-58
Plant D (CE) 49º Nozzle sidehill Axial Stress

Content Deleted – MRP/EPRI Proprietary Material

Figure A-59
Plant D (CE) 49º Nozzle uphill Hoop Stress

Content Deleted – MRP/EPRI Proprietary Material

Figure A-60
Plant D (CE) 49º Nozzle uphill Axial Stress

Content Deleted – MRP/EPRI Proprietary Material

Figure A-61
Plant D (CE) 8º Nozzle downhill Hoop Stress

Content Deleted – MRP/EPRI Proprietary Material

Figure A-62
Plant D (CE) 8º Nozzle downhill Axial Stress

Content Deleted – MRP/EPRI Proprietary Material

Figure A-63
Plant D (CE) 8º Nozzle sidehill Hoop Stress

Content Deleted – MRP/EPRI Proprietary Material

Figure A-64
Plant D (CE) 8º Nozzle sidehill Axial Stress

Content Deleted – MRP/EPRI Proprietary Material

Figure A-65
Plant D (CE) 8º Nozzle uphill Hoop Stress

Content Deleted – MRP/EPRI Proprietary Material

Figure A-66
Plant D (CE) 8º Nozzle uphill Axial Stress

Content Deleted – MRP/EPRI Proprietary Material

Figure A-67
Plant D (CE) ICI Nozzle downhill Hoop Stress

Content Deleted – MRP/EPRI Proprietary Material

Figure A-68
Plant D (CE) ICI Nozzle downhill Axial Stress

Content Deleted – MRP/EPRI Proprietary Material

Figure A-69
Plant D (CE) ICI Nozzle sidehill Hoop Stress

Content Deleted – MRP/EPRI Proprietary Material

Figure A-70
Plant D (CE) ICI Nozzle sidehill Axial Stress

Content Deleted – MRP/EPRI Proprietary Material

Figure A-71
Plant D (CE) ICI Nozzle uphill Hoop Stress

Content Deleted – MRP/EPRI Proprietary Material

Figure A-72
Plant D (CE) ICI Nozzle uphill Axial Stress